



Interactive effect of pre-fermentative grape freezing and malolactic fermentation on the anthocyanins profile in red wines prone to colour instability

Aakriti Darnal^{1,2} · Simone Poggese^{1,4} · Adriana Teresa Ceci^{1,2}  · Tanja Mimmo^{2,3} · Emanuele Boselli^{1,2} · Edoardo Longo^{1,2}

Received: 17 February 2023 / Revised: 13 April 2023 / Accepted: 14 April 2023 / Published online: 7 May 2023
© The Author(s) 2023

Abstract

The effects of pre-fermentative freezing of red grapes from Schiava variety and co-inoculation with lactic bacteria were evaluated on the profile of anthocyanins of the musts and the finished wine. Peonidin-3-glucoside is the main anthocyanin in Schiava grape musts, but it was overcome by malvidin-3-glucoside at bottling. Grape freezing increased the extraction of all anthocyanins in the musts. However, the amount of all anthocyanins except peonidin-3-glucoside and malvidin-3-glucoside was lower in wines from frozen grapes than in control wines. Wines obtained with co-inoculation showed higher anthocyanin content than their respective controls. Petunidin-3-(6''-*p*-coumaroyl)-glucoside, peonidin-3-(6''-*cis-p*-coumaroyl)-glucoside and malvidin-3-(6''-*trans-p*-coumaroyl)-glucoside were dramatically affected by the interaction of the two applied factors. Colorimetric hue (H^*) was strongly correlated with peonidin-3-glucoside, and spectrophotometric tint (N) with malvidin-3-glucoside. Tint also showed a positive correlation with malolactic fermentation.

✉ Adriana Teresa Ceci
AdrianaTeresa.Ceci@unibz.it

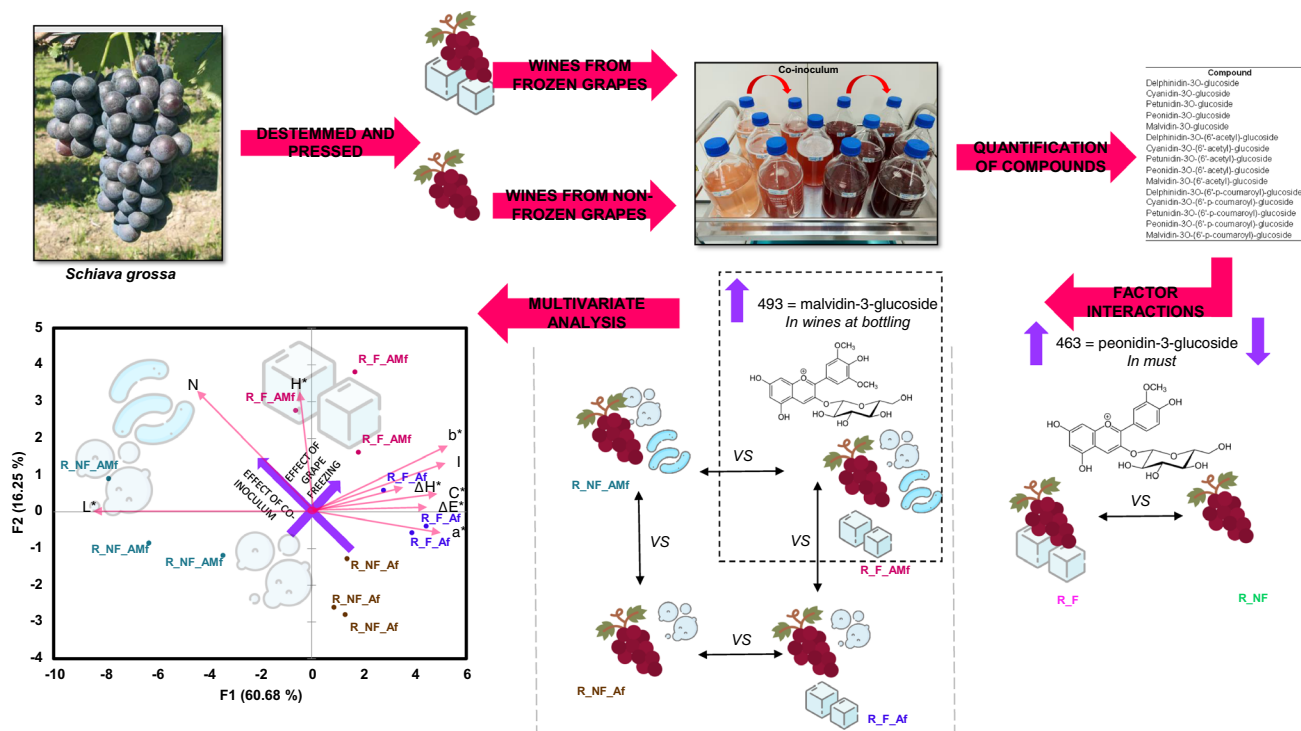
¹ Oenolab–NOI Techpark, Via A. Volta 13, 39100 Bolzano, Italy

² Faculty of Agricultural, Environmental, and Food Sciences, Free University of Bozen-Bolzano, Piazza Università 1, 39100 Bolzano, Italy

³ Competence Centre for Plant Health, Free University of Bolzano, Bolzano, Italy

⁴ Food Experience and Sensory Testing (Feast) Lab, Massey University, Palmerston North 4410, New Zealand

Graphical abstract



Keywords Pre-fermentative grape freezing · Co-inoculum · Anthocyanins · Colorimetry

Introduction

Anthocyanins are among the most important pigments in plants [1]. These polyphenolic compounds are generally responsible for the colour of plants, flowers, and fruits, ranging from orange, pink, red, and violet to blue. More than 500 different distinct natural anthocyanidin-derived compounds have been so far identified, and their profile has been shown to vary considerably from plant to plant [2]. Anthocyanins display antioxidant capacity linked to health-improving properties. Being so widespread in nature and in edible food from plant origin in particular, anthocyanins have always been part of the human diet [3]. Anthocyanin-rich foods have been used historically in traditional medicine, too, for example to treat hypertension, pyrexia, liver disorders, kidney stones, and urinary tract infections, common cold, visual impairment, as well as blood circulation issues. The research in this field is currently investigating the molecular mechanisms of this bioactivity [4, 5].

Red wines and red grapes owe their colour to anthocyanins, although their presence has been established in white grapes as well, even if in traces [6]. Beside their direct effect on wine colour, wine pigmentation due to anthocyanins is also influenced by non-covalent complex formation, i.e.

co-pigmentation, between these and other polyphenolic constituents [7, 8], and by the formation of polymeric pigments during ageing of wines [9]. One main issue influencing the quality of red and rosé wines in terms of colour is indeed their reactivity. For example, anthocyanidin monoglucosides, the main pigments in wines from *Vitis vinifera* cultivars, undergo a complex series of chemical reactions over time, which are dependent on their chemical structure among other factors [10–13]. The most abundant anthocyanin present in most *V. vinifera* sp. grapes and derived wines is usually malvidin-3-glucoside [14]. A study on the chemotaxonomy of grapes applied the anthocyanin profiles in multivariate discriminant analysis to classify the cultivars [14]. However, this is still an ongoing endeavour, aimed also at finding other chemical classes as potential molecular markers for the grapes variety [15]. Grape varieties such as, for example, Cabernet Sauvignon, Merlot, Pinot noir, Cabernet Franc, and Sangiovese (to name some relevant cultivars), all present malvidin-3-glucoside as the most abundant anthocyanin. Other varieties, such as Nebbiolo and the Schiava cultivars (*Schiava grossa*, *Schiava gentile*, *Schiava grigia*, etc.), show instead peonidin-3-glucoside as the most abundant anthocyanin in the grapes. Despite these early findings, chemotaxonomy models built on profiles in grapes might not

be applied directly to the derived wines, since the profile of anthocyanins changes substantially during the winemaking stages and each compound possesses different stabilities and reactivities and extractabilities from the grape skin, depending for instance on their structure substitutions on the B-ring (position and level of hydroxy- and/or methoxylation—see Fig. 1), or the substitution on the glycosidic moiety [16, 17].

Other factors, such as the wine pH and the ability of anthocyanins to form co-pigments with other wine components can also modulate their reactivity. The pH strongly influences the interconversion between different forms of anthocyanidins. At low pH, anthocyanins present a flavylium cation structure (shown in Fig. 1), while at neutral pH uncharged quinone structures can be formed [18]. In alkaline conditions, anthocyanins are less stable and degrade with a loss of coloration. Besides, colourless stable forms can be formed, such as the hydrated hemiketal structure formed in an aqueous environment between pH 4 and 5. Furthermore, the co-pigmentation stabilizes the coloured flavylium cation form at the pH of the wine, at the expense of other forms [7]. Several strategies have been implemented in winemaking to increase the quantity of extracted pigments and polyphenols from grape skins [19]. The techniques applied to increase the extractability of grape polyphenols include cold soaking, freezing with dry ice, or cryomaceration [20]. Studies on Pinot noir cv. vinification has consistently shown that cold soak alone had either no effect or even negative effects on the phenolic composition. Conversely, the application of dry ice, cryomaceration, or freezing of the grape skins/must showed interesting abilities in extracting higher amounts of proanthocyanidins, anthocyanins, or also both, depending on the technique. Overall, there is a consensus that the main mechanism for the increased polyphenols extractability is the breaking of the skin cells of grapes caused by the treatment. Also, other factors, such as the use of

maceration enzymes, have been investigated and showed an improvement in anthocyanins extraction [21]. However, the effect can also be variety dependent. Moreover, the profile of the pigments can be impacted, as the relative amount of malvidin-3-glucoside increased more than that of analogue delphinidin-, cyanidin-, and peonidin-3-glucoside, which decreased with the addition of maceration enzymes.

This study aimed to test the effect of prolonged grape freezing (two weeks) on the profile of anthocyanins in musts and wines, against control samples not subjected to grape freezing. The grapes were from *Schiava grossa* cv. (germ. *Großvernatsch* or *Trollinger*), a *Vitis vinifera* sp. variety used to produce pale red wines. Extraction of more stable anthocyanin components, and/or of higher quantities in general, might improve the intensity and stability of colour over time. Furthermore, the effects induced by co-inoculating malolactic bacteria with yeast have been investigated against control samples in which only yeast was inoculated. A particular focus has also been given to the effects of the interaction of this operation with the applied pre-fermentative cold treatment (grape freezing or not). Malolactic fermentation in wine can impact various properties, such as pH and organic acids content, which in turn could have an impact on wine colour and pigment stability [19–22]. Four types of vinification in triplicates (12 vinification lines in total) were carried out in parallel, according to a 2² full-factorial experimental design. The applied factors were (presence or absence of) (i) grape freezing and (ii) malolactic fermentation, and their interaction. Among them, the vinifications that included the malolactic fermentation without grape freezing are the ones that most closely resemble the winery protocols for vinification of Schiava grapes. In addition, another set of 2² vinification theses in triplicates (12 in total) replicating the same aforementioned conditions, but without application of fermentative maceration on the grape pomace (the protocol

Compound	R1	R2	R3	R4
Delphinidin-3O-glucoside	OH	OH	OH	H
Cyanidin-3O-glucoside	OH	OH	H	H
Petunidin-3O-glucoside	OH	OH	OCH ₃	H
Peonidin-3O-glucoside	OCH ₃	OH	H	H
Malvidin-3O-glucoside	OCH ₃	OH	OCH ₃	H
Delphinidin-3O-(6'-acetyl)-glucoside	OH	OH	OH	acetyl
Cyanidin-3O-(6'-acetyl)-glucoside	OH	OH	H	acetyl
Petunidin-3O-(6'-acetyl)-glucoside	OH	OH	OCH ₃	acetyl
Peonidin-3O-(6'-acetyl)-glucoside	OCH ₃	OH	H	acetyl
Malvidin-3O-(6'-acetyl)-glucoside	OCH ₃	OH	OCH ₃	acetyl
Delphinidin-3O-(6'-p-cumaroyl)-glucoside	OH	OH	OH	p-cumaroyl
Cyanidin-3O-(6'-p-cumaroyl)-glucoside	OH	OH	H	p-cumaroyl
Petunidin-3O-(6'-p-cumaroyl)-glucoside	OH	OH	OCH ₃	p-cumaroyl
Peonidin-3O-(6'-p-cumaroyl)-glucoside	OCH ₃	OH	H	p-cumaroyl
Malvidin-3O-(6'-p-cumaroyl)-glucoside	OCH ₃	OH	OCH ₃	p-cumaroyl
Peonidin-3O-(6'-p-caffeoyl)-glucoside	OCH ₃	OH	H	caffeoyl
Malvidin-3O-(6'-p-caffeoyl)-glucoside	OCH ₃	OH	OCH ₃	caffeoyl

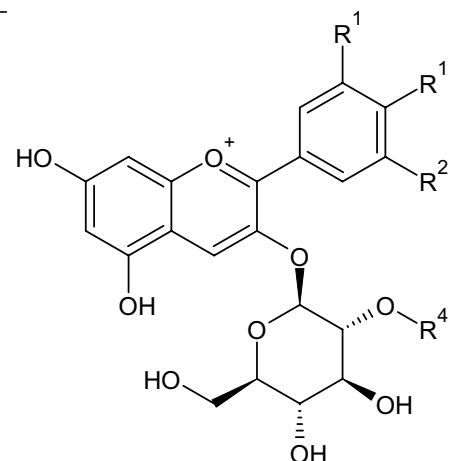


Fig. 1 Main anthocyanin compounds in wine

used for producing white wine), have been briefly compared to the main theses to highlight also the effects of the fermentative maceration.

The effects of the applied factors have been assessed on the anthocyanins composition and the derived pigments, on derived spectrophotometric indexes (colour intensity and hue/tint), and on the colour (measured by CIELab colorimetry) of the produced 12 wine samples (i.e. with and without the application of pre-fermentative grape freezing and of malolactic fermentation).

Finally, the evolution of the identified pigments from freshly pressed must to wine at the end of the fermentation and to the wines at bottling was also discussed to highlight the direct impact of fermentation.

Materials and methods

Grape sampling and laboratory-scale vinifications

Sampling and first processing

Schiava grossa cv. (120 kg) grapes were harvested at technological maturity on October 11, 2021 in Appiano (Bolzano, Italy), in a vineyard exposed northwards. The grapes were carried to the laboratory. 60 kg (samples F) of this mass were immediately put in a freezer at $-20\text{ }^{\circ}\text{C}$ and stored for 14 days.

Of the remaining 60 kg (samples NF):

- 33 kg (samples R_NF) were kept at $+4\text{ }^{\circ}\text{C}$ for one night;
- 27 kg (samples W_NF) were immediately destemmed in a bench crusher and pressed in a pneumatic press (using compressed air to press—pressing in two stages: 0.2–0.5 bar for the first must, followed by 0.5–2.5 bar to maximize extraction).

The basic parameters for the NF and F musts are reported in the Supporting Information (Supporting Information File 1—Table S11).

Treatment of the musts used for red (R) or white (W) vinification

W_NF samples: 16.4 L volume of must was placed in two demijohn glass containers previously sterilized with 5% NaOH solution, followed by a 5% citric acid solution; then, the must was added with $30\text{ mg}\cdot\text{L}^{-1}$ potassium metabisulfite, $50\text{ mg}\cdot\text{L}^{-1}$ of potato protein extract (Vegepure Omnia, HTS Enologia, C.da Amabilina, 218/A, 91025 Marsala, Trapani, Italy), and $30\text{ mg}\cdot\text{L}^{-1}$ of pectolytic enzyme (Enartizym

RS(P), Enatic, via San Cassiano 99, 28069 San Martino, Trecate, No, Italy), followed by $300\text{ mg}\cdot\text{L}^{-1}$ of activated decoloring charcoal (Carbon 100 Plus, HTS Enologia, C/da Amabilina, 218/A–91025 Marsala, Trapani, Italy) as indicated by the technical procedures provided by the producers. The must was then left one night at $+4\text{ }^{\circ}\text{C}$. The next day, the clarified grape juice was taken out and divided into six 2.5 L sterilized borosilicate Duran bottles (2 L must *per* Duran bottle).

R_NF samples: 33 kg non-frozen grapes (R_NF) were destemmed and pressed. The juice was immediately placed in six 2.5 L sterilized Duran bottles (1.8 L juice/Duran bottle) and to each $100\text{ g}\cdot\text{L}^{-1}$ of the removed pressed grape pomace was added.

Inoculum

An aliquot (1.2 L) of the juice was removed from the rest (16.4 L) and placed equally in two 2.5 L sterilized Duran borosilicate bottles, and each Duran bottle was inoculated either with *Saccharomyces cerevisiae* yeast ($40\text{ g}\cdot\text{L}^{-1}$ in total, Fermol DAVIS 522, AEB)—**P1**, or with *Saccharomyces cerevisiae* yeast and an *Oenococcus oeni* malolactic bacteria (EnartisML Silver, Enartis) preparation ($40\text{ g}\cdot\text{L}^{-1}$ of yeast and $40\text{ g}\cdot\text{L}^{-1}$ of malolactic bacteria preparation)—**P2**. Both the yeast and the bacteria were prepared according to the producer's specifications.

The samples were inoculated with either **P1** or **P2** (50 mL *per* Duran bottle), so that W_NF and R_NF were inoculated either with only yeast (W_NF_Af and R_NF_Af) in triplicate, or co-inoculated with yeast and bacteria (W_NF_AMf and R_NF_AMf), also in triplicate. The additions were made so that the final concentration of yeast in each Duran bottle was $1.1\text{ g}\cdot\text{L}^{-1}$ and that of malolactic bacteria preparation (where added) also was $1.1\text{ g}\cdot\text{L}^{-1}$.

W_NF_Af, W_NF_AMf, R_NF_Af, and R_NF_AMf samples: Each prepared Duran bottle without and with added grape pomace (W_NF and R_NF) was then added with $300\text{ mg}\cdot\text{L}^{-1}$ of yeast-activating agent containing thiamine, ammonium sulphate, and dibasic ammonium phosphate (Enovit, AEB, Brescia, Italy), and $50\text{ mg}\cdot\text{L}^{-1}$ of enological gallotannins (Gallovini, AEB, Brescia, Italy) according to the producer's specifications.

Finally, all Duran bottles were added with $30\text{ mg}\cdot\text{L}^{-1}$ of potassium metabisulfite [23]. Each W_NF and R_NF containing bottle was then closed with a perforated cap inserted with a silicon air-stopper closure filled with water, to monitor the production of CO_2 . To be consistent with the most common winemaking procedures adopted by the winemakers [23], fermentation of all W_NF and R_NF theses were carried at $+18\text{ }^{\circ}\text{C}$ and at $+25\text{ }^{\circ}\text{C}$, respectively.

Fermentation

R_NF: 3 days and 8 days after the inoculum, 30 mg·L⁻¹ of potassium metabisulphite was added to all Duran bottles. 200 mg·L⁻¹ of diammonium phosphate (HTS Enologia) was added to all samples 3 days and 4 days after the inoculation. On the 5th day, 300 mg·L⁻¹ of Enovit were added. The fermentation ended after 10 days for R_NF samples. These were then racked and added with 15 mg·L⁻¹ of potassium metabisulphite. After another 5 days, all R_NF samples were cooled down to +6 °C, added with one Antiflor tablet (Enartis), 40 mg·L⁻¹ of potassium metabisulphite, and 250 mg·L⁻¹ of enological tannins (Fermotan SG, AEB) according to the producer's specifications.

W_NF: The fermentation ended after 20 days for W_NF samples and one Antiflor tablet (Enartis) 120 mg·L⁻¹ of potassium metabisulphite was added.

Samples from frozen grapes

After 2 weeks at -20 °C, the frozen grapes (for F samples) were left at +4 °C for 2 days to defrost and then they processed exactly as herein described for the non-frozen (NF) grapes samples (paragraphs 2.1.1 to 2.1.4).

Stabilization and bottling

The stabilization of all produced wines was performed by keeping the samples at +4 °C for 2 months. Exactly on the 48th day after the inoculum (beginning of the fermentation), all samples were added with 120 mg of sodic bentonite (Bent Gold, HTS Enologia) after its pre-activation

(according to the producer). The samples were left to stabilize for another 14 days, after which the clarified liquid was transferred to another sterilized container and added with 50 mg·L⁻¹ of potassium metabisulphite. Considering all losses due to the transfers, the final volumes for all (W) samples were about 1.8 L, and for all R samples about 1.6 L. After overall 2 months, all samples were filtered under gravity in sterilized dark-brown 750-mL wine bottles over Whatman filter papers and under a gentle N₂ flow. All bottles were sealed with a cork stopper and externally further sealed with sealing wax. Two bottles per Duran container were thus obtained, producing overall 8 these × 3 replicates × 2 samples = 48 bottles. All samples were then labelled according to the different type/thesis, and stored at 4 °C in darkness. The sample theses produced in this study are summarized in Fig. 2. In regard to the aim of this article, the red (R) vinification was highlighted to gain insight of all the investigated factors and their interactive effects in the evolution of anthocyanins from must to wine. Furthermore, vinifications without fermentative maceration (W—white samples) were prepared in parallel to study the effect of the fermentative maceration over the pre-fermentative and inoculum-type factors.

LC-MS/MS analysis of anthocyanins

The analysis of anthocyanins was conducted according to Favrea et al. [24]. An aliquot (2 mL) of each sample was filtered with a Corning syringe filter (0.2 µm pore size, 1.5 cm diameter) before each analysis. The LC-MS analyses of anthocyanins and derived compounds were performed on a UHPLC-QqQ/MS instrument (Agilent

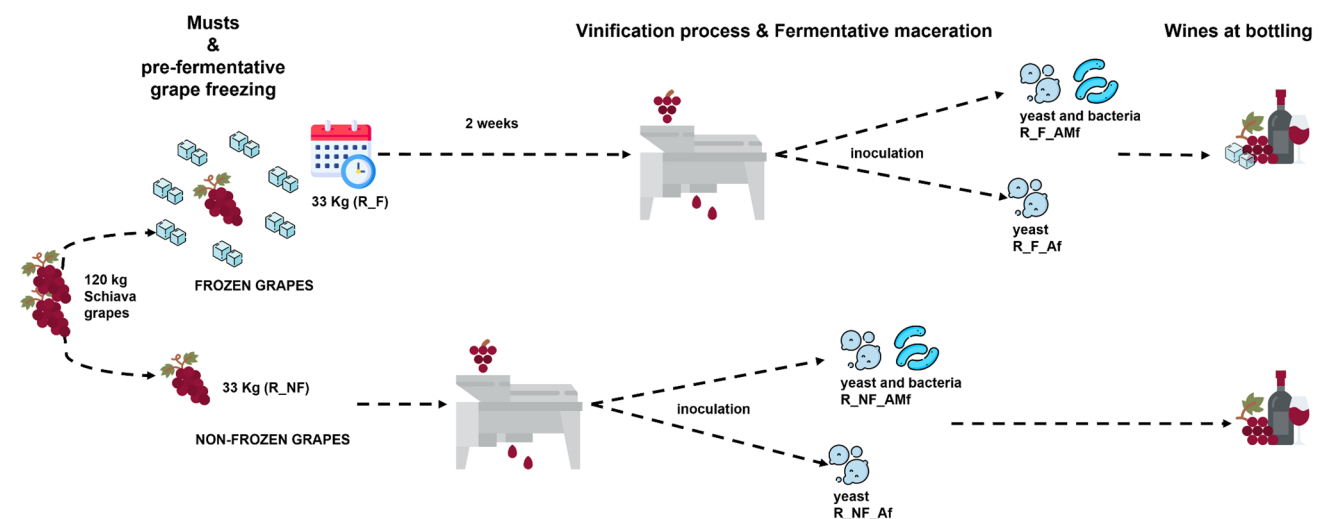


Fig. 2 Protocol for red (R) vinification. R, samples obtained with fermentative maceration of grape pomace; NF, without pre-fermentative grape freezing; F, with pre-fermentative grape freezing; Af, inoculum

of only yeast; AMf, co-inoculum of yeast and malolactic bacteria. Only R samples were investigated in this study

LC/TQ 6465 system) equipped with a 1260 Infinity II UHPLC with a quaternary pumps system, a 1260 Infinity II WR PDA detector, in series to a AJS (ESI)-QqQ-MS mass analyzer. The chromatographic separations were carried out on a Poroshell 120, SB-C18 2.1 mm × 100 mm × 2.7 μm (Agilent Technologies Italia S.p.A. Cernusco sul Naviglio, MI at 30 °C with 0.35 mL min⁻¹ flow rate. The mobile phase consisted of A) 4.5% formic acid in degassed ultrapure water, and B) 4.5% formic acid in acetonitrile. All used solvents and mobile phase additives were of MS grade. The gradient separation programme was as follows: 5%B from 0 to 1 min, 5 to 15%B from 1 to 10 min, 15 to 25%B from 10 to 15 min, 25 to 40%B from 15 to 18 min, 40 to 95%B from 18 to 21 min, 95%B from 21 to 24 min, 95 to 5%B from 24 to 25 min, 5%B from 25 to 28 min. The PDA detector was set to record absorbances in the 200–700 nm wavelength range using a 4 s response time (1.25 Hz) and 4 nm slit width, with 1 nm spectrum steps. The MS detection was carried in ESI+ ionization mode, with the following applied parameters: mass range = *m/z* 200–700, scan time = 500 ms, step size = 0.1 amu, fragmentor potential = 135 V, cell acceleration = 5 V, N₂ gas temperature = 340 °C, N₂ gas flow = 13 L min⁻¹, nebulizer pressure = 50 psi, sheath gas heater = 350 °C, sheath gas flow = 12 L min⁻¹, capillary voltage = +3500 V, nozzle voltage = +1000 V. MS² analyses of selected precursors were carried at collision energy = 30 eV (CID), unless stated otherwise in the text. FullMS raw data were converted into .mzData format and exported from MassHunter qualitative software for data analysis (Agilent). MzMine3 (<http://mzmine.github.io/>) application was employed for automatic alignment of the exported data and their pre-processing. The peak table features were finally selected manually inspecting the correspondence with peaks in the 500–550 nm UV–Vis absorption range, from the acquired PDA chromatograms (maximum absorbance range for anthocyanins). MS retention times were corrected for the retention times of the PDA traces (which was just flow rate dependent), i.e. $Rt^{MS} - Rt^{PDA} = +0.1$ min, employing reference signals. Compound semi-quantitation was obtained against the calibration of malvidin chloride reference standards (ESI+ measured mass = *m/z* 331.1; retention time = 14.6 min) by linear regression (linear calibration range = 0.1–1 g·L⁻¹, regression adj.-*R*² = 0.988, regression slope = 3,989,039, area·g⁻¹·L, regression intercept set to 0).

Spectrophotometric analysis

All wine samples were analysed on a single/beam UV-1200 spectrophotometer. The measurement spectral range was 650–250 nm, using 2 mm-width quartz

cuvettes), a *D*_{nm} = 1 measuring interval, and normal acquisition speed. The collected original data are available in the Supporting Information (Supporting Information—Table SI2). Data were corrected for baseline effects by subtracting the absorbance measured at 650 nm from all absorbance values.

The chromatic characteristics were calculated according to the OIV protocols [25, 26]. Accordingly, the following derived parameters were calculated:

Colour intensity = $A_{420} + A_{520} + A_{620}$, where the *A* values (absorbance) were converted for a 1 cm pathlength.

$$\text{Hue/Tint } N = \frac{A_{420}}{A_{520}}$$

CIELab colorimetric analysis

Colour parameters *L*^{*}, *a*^{*}, *b*^{*} (CIE, 1986) were recorded using a reflectance spectrophotometer Minolta CR-400 Chroma Meter (Minolta Corp., Osaka, Japan). The instrument was calibrated over the provided white ceramic plate. ΔE_{ab}^{*} colour difference from the reference was calculated as

$\Delta E_{ab}^{*} = \sqrt{(\Delta a^{*})^2 + (\Delta b^{*})^2 + (\Delta L^{*})^2}$. Besides, the following parameters were derived following the OIV published guidelines [27]:

$$\text{Chroma (chromaticness)} : C^{*} = (a^{*2} + b^{*2})^{1/2};$$

$$\text{Tone (in degrees)} : H^{*} = \text{tg}^{-1}(b^{*}/a^{*});$$

$$\text{Difference in tone} : \Delta H^{*} = [(\Delta E^{*})^2 - (\Delta L^{*})^2 - (\Delta C^{*})^2]^{1/2}$$

Basic enological parameters

Basic enological parameters were determined on a MIURA One automatic analyser (Exacta + Optech Labcenter SpA, San Prospero, Modena, Italy) for L-tartaric acid, L-malic acid, L-lactic acid, glucose, and fructose, α-amino nitrogen (total amino acids), free ammonium, total sulphur dioxide, free sulphur dioxide, and total polyphenols. Each parameter was calibrated on the relative reference standard provided by the supplier. The alcohol content (%EtOH, v/v) was determined by distillation followed by electronic densimetry, according to OIV protocols [28]. The pH was measured on an XS pH 60 VioLab benchtop pH meter (XS Instruments, Carpi, Italy) previously calibrated at pH 7.0 and 4.0. The basic enological parameters in wines at bottling are expressed as averages over three replicates and their related standard deviations; these data are reported in the Supporting Information (Supporting Information—Table SI1).

Statistical analysis

All the statistical analysis and the related graphics were performed in XLstat (Addinsoft, 40, rue Damrémont, 75018 PARIS). For ANOVA with Tukey's HSD post hoc test, the statistical significance was set at $\alpha = 0.05$, unless otherwise

specified. For all principal component analysis (PCA), variables were first auto-scaled (mean-centring followed by scaling by standard deviation, calculated using the $n-1$ denominator) before calculation of the model, unless stated otherwise.

Table 1 Anthocyanins of Schiava

Assignment	MS ¹ ion—ESI + (± 0.1 m/z)	Average Rt (± 0.1 min)	UV–Vis λ_{\max} (± 1 nm)	MS ² precursor (± 0.1 m/z)	CID (eV)	MS ² product ions (± 0.1 m/z) [relative abundance %]	Refs.
<i>Not assigned</i>	485.1	5.4	533	485.1	40	485[73.1];353[9.6];166[1.9];102.3[2];101.7[9.6];39[3.7]	
Delphinidin-3-glucoside	465.0	6.2	525	465.0	30	465[3.1];303[92.4];187[1.7];39[2.9]	(a)
Cyanidin-3-glucoside	449.0	7.5	515	449.0	30	287[98.9];70[1.1]	(a)
Petunidin-3-glucoside	479.0	8.5	527	479.0	30	317[96.9];302[3.0]	(a)
Peonidin-3-glucoside	463.0	9.8	517	463.0	30	301[95.4];286[4.6]	(a)
Malvidin-3-glucoside	493.1	10.5	528	493.1	30	331[97.8];316[1.0];315[1.1]	(a)
Vitisin A	561.0	11.4	521	561.0	30	399[100]	[29, 30]
<i>Not assigned</i>	619.1	12.0	*	619.1	20	619.1[79.7];353.0[1.9];39.1[18.3]	
<i>Not assigned</i>	619.1	12.3	*	619.1	20	619.0[73.6];150.8[0.8];39.1[25.6]	
Cyanidin-3-(6''-acetyl)-glucoside	491.1	12.9	518	491.1	30	287[100]	(a)
Petunidin-3-(6''-acetyl)-glucoside	520.7	13.3	*	520.7	40	317[86.0];305[7.0];302[3];45[4]	[31]
Malvidin-3-glucoside vinyl(epi)catechin**	475.1 (643.1; 491.1)	13.8	*	475.3	65	475[82.2];457[10.1];247[3.3];35[1.3];123[1.2];39[1.9]	[32, 33]
Peonidin-3-(6''-acetyl)-glucoside	505.1	14.5	520	505.1	30	301[98.6];286[1.4]	[31]
Malvidin-3-(6''-acetyl)-glucoside	535.1	14.8	531	535.1	30	331[100]	[31]
Peonidin-3-(6''-caffeoyl)-glucoside	625.1	15.2	523	625.1	30	301[100]	[31]
Petunidin-3-(6''-p-coumaroyl)-glucoside	625.1	15.7	*	625.1	30	625[15.4];317[84.6]	[31]
Peonidin-3-(6''-cis-p-coumaroyl)-glucoside	609.0	15.9	521	609.0	30	301[100]	[31]
Malvidin-3-(6''-cis-p-coumaroyl)-glucoside	639.1	16.1	*	639.1	30	639[2.9];331[97.1]	[31]
Peonidin-3-(6''-trans-p-coumaroyl)-glucoside	609.1	16.7	522	609.1	30	301[100]	[31]
Malvidin-3-(6''-trans-p-coumaroyl)-glucoside	639.1	16.8	533	639.1	30	331[100]	[31]

Retention times (min) are reported for the aligned dataset and indicate the average deviation from the mean. The shown average retention times are corrected for the corresponding PDA retention times

^a<https://mona.fiehnlab.ucdavis.edu/>

*Peak too small, close to background noise

**Base mass (reported in the table) would be an in-source fragment of the precursor m/z 643.1

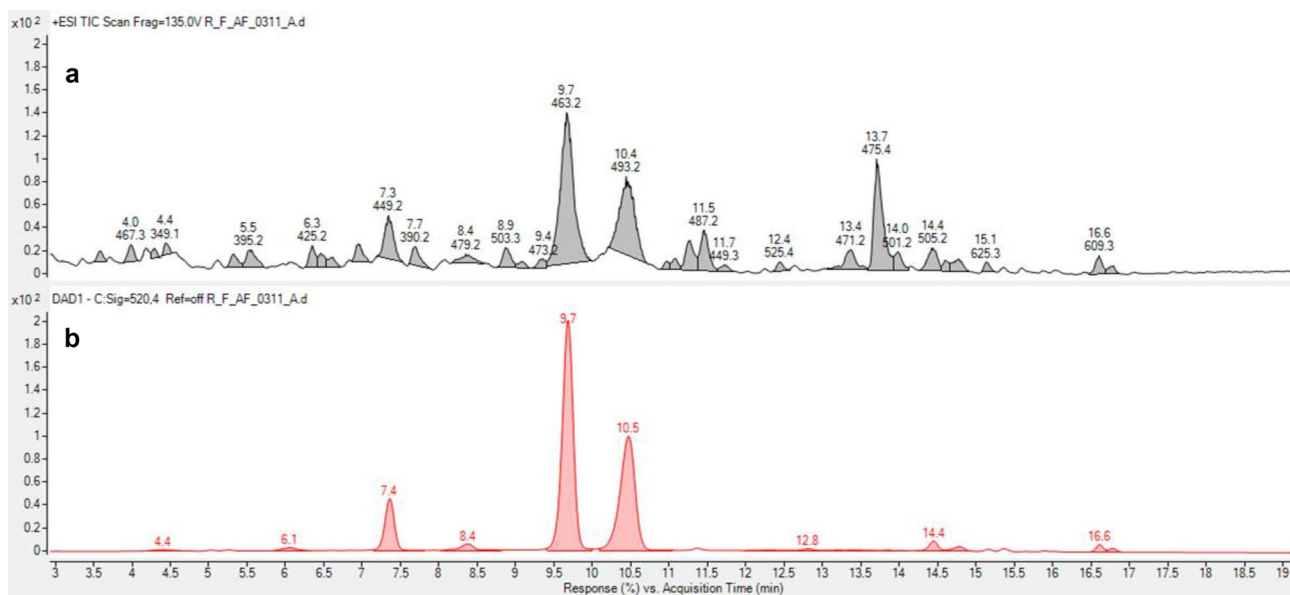


Fig. 3 **A** Total ion chromatogram (TIC) full MS trace indicating the retention times and associated base peaks, **B** parallel PDA trace extracted at 520 nm. MS retention times were corrected for the PDA retention times. Note: in the figure, the shown retention times are cor-

rected for the alignment between PDA and TIC traces; these might not coincide with the one reported in Table 1, as those retention times were averaged over all acquired samples

Results and discussion

Identified anthocyanins and derived pigments

The list of all identified compounds is reported in Table 1. MS² spectra traces are reported in Supporting Information—MS² spectra. The generic profile of anthocyanins is reported in Fig. 3.

The PDA traces were employed to identify pigment compounds according to their absorption at 520 (± 4) nm (Table 1). The assignment of most compounds detected in MS¹ analysis was confirmed by target MS² analysis. All major wine monoglucosidic anthocyanins were identified. In addition, acetyl-glucosidic, *p*-coumaroyl-glucosidic, and caffeoyl-glucosidic derivatives of peonidin and malvidin (the two main Schiava anthocyanidins) were identified [31], including *cis* and *trans* isomers of the *p*-coumaroyl-glucosides. The species m/z 485.1 at 5.4 min could not be assigned. The species m/z 475.1 appeared in MS¹ along with a higher m/z 491.1, although much smaller; accordingly, this species was assigned to malvidin-3-glucoside vinylcatechin or malvidin-3-glucoside vinelepicatechin, according to Hayasaka et al. [32] and Francia-Aricha et al. [33]. The actual precursor m/z 643 could not be observed, possibly due to a complete in-source fragmentation. Although this was the most likely assignment, this species has not been further applied for the statistical analysis of the obtained results.

The two species at m/z 619 also could not be assigned and likewise not applied for further discussion. The final peak tables used for the statistical analyses are reported in the Supporting Information—Table SI3.

Anthocyanin evolution from the musts to wines at bottling

To study the effects of the pre-fermentative treatment (NF=no grape freezing *versus* F=grape freezing) in musts, differences in the anthocyanin abundances were investigated by 1-way ANOVA with Tukey's HSD post hoc test (confidence limit at $\alpha = 0.05$). The results are presented in Table 2.

449 cyanidin-3-glucoside, 463 peonidin-3-glucoside, 465 delphinidin-3-glucoside, 479 petunidin-3-glucoside, 491 cyanidin-3-(6''-acetyl)-glucoside, 493 malvidin-3-glucoside, 505 peonidin-3-(6''-acetyl)-glucoside, 521 petunidin-3-(6''-acetyl)-glucoside, 535 malvidin-3-(6''-acetyl)-glucoside, 561 vitisin A, 609-1 peonidin-3-(6''-*cis*-*p*-coumaroyl)-glucoside, 609-2 peonidin-3-(6''-*trans*-*p*-coumaroyl)-glucoside, 625-1 peonidin-3-(6''-caffeoyl)-glucoside, 625-2 petunidin-3-(6''-*p*-coumaroyl)-glucoside, 639-1 malvidin-3-(6''-*cis*-*p*-coumaroyl)-glucoside, 639-2 malvidin-3-(6''-*trans*-*p*-coumaroyl)-glucoside; R musts that did not undergo overnight clarification (and that were used later for vinification with fermentative maceration), F frozen grapes, NF non-frozen grapes. Determinations were done in duplicates

Table 2 Results of one-way ANOVA and Tukey's HSD for musts

Pre-fermentative treatment (B)	465	449	479	463	493	561	491	521	505	535	625-1	625-2	609-1	639-1	609-2	639-2
F	3.750b	34.500a	8.925b	205.075b	52.925b	0.050a	3.000b	0.725 a	16.800b	7.350a	0.950b	0.450a	3.000 b	1.100a	16.450b	4.375a
NF	1.900a	19.467a	3.883a	95.717 a	27.917a	0.200b	0.767a	9.367 b	8.233 a	3.100a	0.383a	0.517a	1.167 a	0.650a	2.567 a	7.267b
Pr > F(B)	0.005	0.126	0.028	< 0.0001	0.024	0.019	0.006	< 0.0001	0.001	0.078	0.002	0.261	< 0.0001	0.131	0.000	0.020
Significant	Yes	No	Yes	Yes	Yes	Yes	Yes	Yes	Yes	No	Yes	No	Yes	No	Yes	Yes

ANOVA results for musts (Table 2) highlight the dependence of the anthocyanins profile on the applied variables. The effect of the pre-fermentative treatment (grape freezing) on the anthocyanins profile appeared clearly in the musts.

All major species with significant differences were more concentrated in the F samples, in agreement with previous studies on the effect of grape freezing on extraction [19]. Exceptions were vitisin A (561), petunidin-3-(6''-acetyl)-glucoside (521), and malvidin-3-(6''-trans-*p*-coumaroyl)-glucoside (639-2), with a higher concentration in the NF must samples instead.

For wines at bottling, the effects of pre-fermentative treatment (NF—no grape freezing *versus* F—grape freezing) and the type of inoculum (Af—only yeast *versus* Amf = yeast + malolactic bacteria), including their interactions, were investigated in wines by two-way ANOVA with Tukey's HSD post hoc test (confidence limit at $\alpha = 0.05$). These results are presented in Table 3.

The same effect of the pre-fermentative treatment previously observed in musts was still present for peonidin-3-glucoside only, while the other main anthocyanin, malvidin-3-glucoside, did not show significant differences in wine at bottling (Table 3). Interestingly, most of the other minor components actually had higher values in wines from non-frozen grapes (NF). This might appear as a counterintuitive result, especially in view of the absence of noticeable interactions: peonidin-3-glucoside aside, most compounds that were significantly more concentrated in musts from frozen grapes, were instead significantly higher in wines from non-frozen grapes. Concerning specifically the effect of malolactic fermentation, this caused a significant increase in the content of anthocyanins in wine. In no case the opposite was observed.

The found results confirm knowledge from previous literature on the effect of grape freezing on must composition [19]. Besides, the main anthocyanins in Schiava (peonidin-3-glucoside and malvidin-3-glucoside) were relatively more concentrated in F wine samples (although this was a trend only for malvidin) than in NF samples, regardless of the type of fermentation (Table 3). It is also interesting to note that the relative change from must to wine occurred depending on the pre-fermentative treatment (grape freezing) of the grape and the type of inoculum.

Very interestingly, a peculiar observation with regard to the concentration ratio values in musts and wines for the compound couples cyanidin-3-glucoside/petunidin-3-glucoside (449/479) and peonidin-3-glucoside/malvidin-3-glucoside (463/493) is worth noticing. In musts from frozen grapes (F), the concentration ratio values (Table 2) between the couples 449/479 and 463/493 are strikingly identical (ratio = 3.88). These results are consistent in their relative F wines at bottling (Table 3) and these ratios were closer to 1 (cyanidin-3-glucoside/petunidin-3-glucoside = 1.06) or even

Table 3 Results of the two-way ANOVA and Tukey's HSD for wines

Pre-fermentative treatment (B)	465	449	479	463	493	561	491	521	505	535	625-1	625-2	609-1	639-1	609-2	639-2
F	1.000a	4.433a	4.183a	31.317b	32.550a	0.250a	0.933a	0.250a	5.817a	2.533a	0.783a	0.317a	1.100a	0.317a	8.000a	4.567a
NF	1.800b	5.617a	4.967b	24.883a	30.767a	0.150a	1.150a	0.433b	5.000a	3.983b	0.383a	0.650b	1.633b	0.600b	10.350b	6.683b
Pr > F(B)	< 0.0001	0.234	0.031	0.004	0.436	0.511	0.437	0.003	0.425	0.002	0.119	0.004	0.000	0.011	0.008	0.000
Significant	Yes	No	Yes	Yes	No	No	No	Yes	No	Yes	No	Yes	Yes	Yes	Yes	Yes
Type of inoculum (C)	465	449	479	463	493	561	491	521	505	535	625-1	625-2	609-1	639-1	609-2	639-2
AMf	1.650b	7.000b	5.117b	32.050b	34.833b	0.267a	1.233a	0.400b	6.450b	3.467a	0.817b	0.600b	1.567b	0.517a	10.733b	6.650b
Af	1.150a	3.050a	4.033a	24.150a	28.483a	0.133a	0.850a	0.283a	4.367a	3.050a	0.350a	0.367a	1.167a	0.400a	7.617a	4.600a
Pr > F(C)	0.002	0.003	0.007	0.001	0.019	0.386	0.186	0.029	0.064	0.217	0.076	0.023	0.002	0.215	0.002	0.001
Significant	Yes	Yes	Yes	Yes	Yes	No	No	Yes	No	No	No	Yes	Yes	No	Yes	Yes
B* C	465	449	479	463	493	561	491	521	505	535	625-1	625-2	609-1	639-1	609-2	639-2
NF* AMf	2.133c	7.833b	5.733b	28.467bc	34.333a	0.267a	1.600a	0.500b	6.700a	4.533c	0.400a	0.900b	1.967c	0.733b	12.567b	8.367c
F* AMf	1.167b	6.167ab	4.500ab	35.633c	35.333a	0.267a	0.867a	0.300a	6.200a	2.400a	1.233a	0.300a	1.167ab	0.300a	8.900a	4.933ab
NF* Af	1.467b	3.400a	4.200a	21.300a	27.200a	0.033a	0.700a	0.367ab	3.300a	3.433bc	0.367a	0.400a	1.300b	0.467ab	8.133a	5.000b
F* Af	0.833a	2.700a	3.867a	27.000b	29.767a	0.233a	1.000a	0.200a	5.433a	2.667ab	0.333a	0.333a	1.033a	0.333ab	7.100a	4.200a
Pr > F(B* C)	0.166	0.614	0.171	0.665	0.728	0.511	0.087	0.715	0.212	0.059	0.095	0.013	0.015	0.122	0.085	0.008
Significant	No	No	No	No	No	No	No	No	No	No	No	Yes	Yes	No	No	Yes

449 cyanidin-3-glucoside, 463 peonidin-3-glucoside, 465 delphinidin-3-glucoside, 479 petunidin-3-glucoside, 491 cyanidin-3-(6''-acetyl)-glucoside, 493 malvidin-3-glucoside, 505 peonidin-3-(6''-acetyl)-glucoside, 521 petunidin-3-(6''-acetyl)-glucoside, 535 malvidin-3-(6''-acetyl)-glucoside, 561 vitisin A, 609-1 peonidin-3-(6''-cis-p-coumaroyl)-glucoside, 609-2 peonidin-3-(6''-trans-p-coumaroyl)-glucoside, 625-1 peonidin-3-(6''-caffeoyl)-glucoside, 625-2 petunidin-3-(6''-p-coumaroyl)-glucoside, 639-1 malvidin-3-(6''-cis-p-coumaroyl)-glucoside, 639-2 malvidin-3-(6''-trans-p-coumaroyl)-glucoside; R wines obtained with fermentative maceration, F frozen grapes, NF non-frozen grapes, Af inoculum with only yeast, Amf co-inoculum of yeast and malolactic bacteria

lower (peonidin-3-glucoside/malvidin-3-glucoside = 0.96). Again regarding musts, as a direct consequence, an identical ratio was found also between the couples 463/449 and 493/479 (ratio = 5.9).

The unexpected coincidence between the four glucosidic species with regard to their concentration ratios in the F musts could be explained directly by their *prior* relative abundances in grapes. Indeed, we could also add that the structural difference between cyanidin and petunidin is exactly the same as the one between peonidin and malvidin, i.e. an extra methoxyl substitution on the B-ring [30]. Then, peonidin presents an hydroxyl and a methoxyl moiety on the B-ring, in place of the two hydroxyl units of cyanidin; an analogous observation could be made for the difference in structure between malvidin and petunidin. Our results showed that the application of grape freezing, as a pre-fermentative treatment, could directly translate the composition in grape into the composition of all these four glucosidic species in the musts. Grape freezing might have completely overcome the differences in extractability of these four compounds from frozen grapes into the musts, revealing the concentration ratios they had in the grapes. Indeed, it is well known that the content and presence of specific anthocyanins was given by the pathway that occurred and the abundance of specific precursors [31]. On the contrary, this observation was not made in musts from non-frozen grapes (NF, Table 2): in NF musts, the 449/479 ratio was ~5, whereas the 463/493 ratio was ~3.4. The difference in the two ratios in NF musts might be due to a difference in the extractability of 449 vs 463 and 479 vs 493, i.e. so fully showing the effect of the relative extractabilities of the four species that depends on the substitution on the B-ring [30]. To complete the description of the evolution of the anthocyanins profile from must to wine, in Fig. 4 the plot of the LS

means with the associated significances for the third-order interaction term ($T*B*C$) between time (T =time, R musts vs R wines only), factor B (pre-fermentative grape freezing vs no grape freezing), and factor C (type of inoculum) is reported together with the associated Tukey’s HSD-related grouping letters. The LS mean values have been scaled, to present an easier way to visualize all the results in a unique plot.

The scaled LS means comparison allows appreciating how the highest value for almost all species of anthocyanins was reached in the musts from frozen grapes (pink-dashed bars). This is evidenced as a trend, even in those cases where the change from must to wine was not significant (e.g. 479—petunidin-3-glucoside, 493—malvidin-3-glucoside, 535—malvidin-3-(6''-acetyl)-glucoside).

Regarding anthocyanin glucosides (449—cyanidin, 463—peonidin, 465—delphinidin, 479—petunidin), all showed similar trends in this respect, with the lowest values in wines from frozen grapes that underwent alcoholic fermentation only (Af)—blue bars. However, the trend was not present for peonidin-3-glucoside (463), as the NF_Af samples were the ones showing the lowest content. On the contrary, the anthocyanin derivatives, characterized by complex patterns of glycosylation, acetylation, and acylation (491—cyanidin, 505—peonidin, 521—petunidin, 535—malvidin) displayed diverse trends depending on the species. Petunidin acetylglucoside (521) in particular showed the highest concentration in NF musts and the lowest in F wines (regardless of the type of inoculum).

Anthocyanins *p*-coumaroylated derivatives also did not display a specific common trend. Notably, comparing *cis* and *trans* *p*-coumaroyl-glucoside derivatives, malvidin showed an increase from must for the *trans* 639-2 isomer in the NF_AMf samples and a decrease for the *cis* 639-1 isomer in all

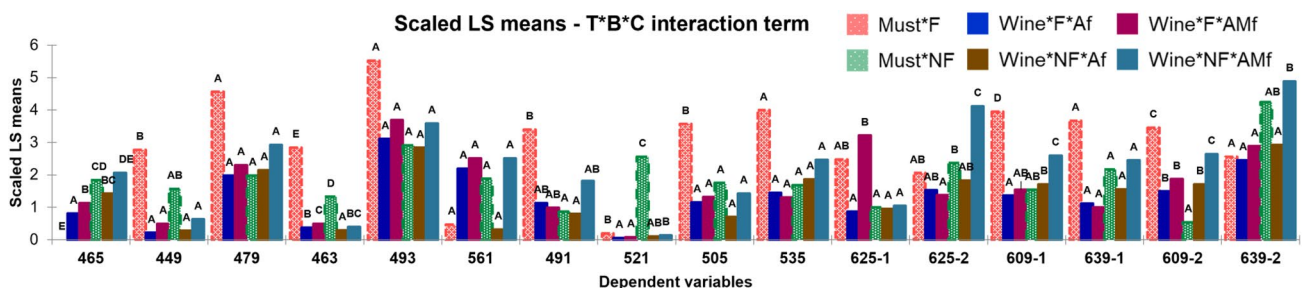


Fig. 4 Scaled LS means from three-way ANOVA analysis for the three-factor interaction term. Before plotting, LS mean values for the same compound were scaled (to unit standard deviation) to improve visualization. Grouping letters are, however, still reported for the original LS mean values. Concentration values are reported against malvidin chloride (MvCl) calibration. Dashed lines are used to indicate LS means of must samples. 449 cyanidin-3-glucoside, 463 peonidin-3-glucoside, 465 delphinidin-3-glucoside, 479 petunidin-3-glucoside, 491 cyanidin-3-(6''-acetyl)-glucoside, 493 malvidin-

3-glucoside, 505 peonidin-3-(6''-acetyl)-glucoside, 521 petunidin-3-(6''-acetyl)-glucoside, 535 malvidin-3-(6''-acetyl)-glucoside, 561 vitisin A, 609-1 peonidin-3-(6''-cis -*p*-coumaroyl)-glucoside, 609-2 peonidin-3-(6''-trans-*p*-coumaroyl)-glucoside, 625-1 peonidin-3-(6''-caffeoyl)-glucoside, 625-2 petunidin-3-(6''-*p*-coumaroyl)-glucoside, 639-1 malvidin-3-(6''-cis-*p*-coumaroyl)-glucoside, 639-2 malvidin-3-(6''-trans-*p*-coumaroyl)-glucoside; F frozen grapes, NF non-frozen grapes, Af inoculum with only yeast, AMf co-inoculum of yeast and malolactic bacteria

cases, whereas the peonidin-containing analogues did not. Indeed, coumaroylated peonidin derivatives showed the the lowest absolute amount for the *trans* isomer 609-2 in the NF must, whereas the highest was the *cis* 609-1 in the F musts. Both compounds, 609-1 and 609-2, increased from must to wines in NF samples.

It is known that sunlight and UV light induce isomerization of the *trans* isomer into the *cis* isomer of *p*-coumaroyl-glucoside derivatives. In this case, the different amount of *cis* or *trans* *p*-coumaroyl-glucosidic derivatives in F and NF musts was most likely due to a spontaneous conversion of the two isomers [34], as the must and wine samples did not undergo UV light exposure; besides, the fermentation and subsequent cold stabilization stages occurred in complete darkness.

Finally, vitisin A was identified in all samples and showed to drop considerably from must to wine only in NF_Af samples, whereas in all other cases either did not change significantly (NF_AMf) or even increased from the must to wine (F samples). Indeed, these effects might be caused by the fermentation or by later stages (e.g. cold stabilization).

For musts and wines subjected to alcoholic fermentation alone (Af) and co-inoculum of yeasts and malolactic bacteria (AMf), the concentration ratio values for compound couples 449/479 vs. 463/493 and for couples 463/449 vs. 493/479 were analysed. The samples of wines_F_Af showed that the concentration ratio values (Fig. 4) between the 449/479 and 463/493 couples were surprisingly identical (ratio=0.71 and 0.91, respectively). The concentration ratios in wines_F_AMf were closer to 1 (449/479=1.36) or even lower (463/493=0.99). In both wines_F_Af and wines_F_AMf samples, different concentration ratios were found between the couples 463/449 (10.00 and 7.81, respectively) and 493/479 (5.83 and 7.84, respectively), thus showing that the fermentation processes changed the ratios between these four species. It is well known that dihydroxy pigments are more unstable than the anthocyanins characterized by hydroxyl and a methoxyl moieties on the B-ring; furthermore, the anthocyanin profile depends on the variety [31]. The differences between these concentration ratios in wines could be attributed to the fact that the application of fermentation processes had a profound effect on the content of these four pigments, thus affecting the variability of anthocyanin content in wines. With regard to wines from non-frozen grapes, only the wines_NF_Af samples showed an interesting trend. The concentration ratios (Fig. 4) between couples 449/479 vs. 463/493 (ratio=0.81 and 0.78, respectively) and couples 449/479 vs. 463/493 were similar (ratio=6.29 and 6.47, respectively).

To better visualize the direct effect of the fermentation process, the time evolutions from must to bottling (including the values at the end of the fermentations) for each investigated sample have been included in the Supporting

Information—Table SI4. These plots are also supported by the Tukey's HSD test results, presented in the same Table SI4 (tested for these time evolutions *per* each sample). Most compounds underwent the fastest drop over the fermentation stage, with a few exceptions. The two major pigments, peonidin-3-glucoside and malvidin-3-glucoside, underwent rather different fates over the process. Peonidin-3-glucoside (463) showed a drop in all samples over the fermentation, with relatively faster rates in F wines, probably due to the highest initial concentrations [21] it had in the related musts, whereas malvidin-3-glucoside (493) showed a steady level or even an increase over the fermentation in the case of R_NF_AMf, with a subsequent decrease. Delphinidin-3-glucoside (465) showed markedly different trends for F and NF samples, with a relative drop over the fermentation for the F samples, which was absent (R_NF_Af) or even reversed (R_NF_AMf) in the case of the NF samples. Cyanidin-3-glucoside (449) showed a decrease over all the vinifications and a stable value after that point up to the bottling in all cases. Dramatic effects due to the applied conditions were observed for some derived species. Vitisin A (561) did not show any increase during the fermentation for the F samples, whereas it increased substantially in the NF samples. Also interesting was its fate after the end of the fermentation, with a sharp increase in F samples and a relative drop in NF samples. The trends for other derived compounds were also strongly sample dependent. Peonidin-3-(acetyl)-glucoside displayed a relatively small or insignificant drop over the fermentation in F samples, whereas it dropped considerably for R_NF_Af samples. Its malvidin analogue (535) had a relatively non-significant drop only after the end of the fermentation in F samples, with no significant change over the fermentation, whereas in NF samples its content increased in NF samples, to then go back to values closer to the ones in must. Even more drastic was the difference between F and NF samples of peonidin-3-(*p*-coumaroyl)-glucoside (609-1 and 609-2, for *cis* and *trans* isomers, respectively). In F samples, the *cis* isomer showed a faster decrease up to the end of the fermentation than its *trans* isomer; instead, in the NF samples, both compounds increased overall, either over the fermentation (*cis* isomer) with a subsequent small drop, or afterwards (*trans* isomer).

Overall, the two main anthocyanins (peonidin-3-glucoside and malvidin-3-glucoside) underwent rather different evolutions from must to wine at bottling. To highlight this discrepancy, in the Supporting Information (Supporting Information—Table SI5), the percentage of the leftover compounds in wine with respect to must for all identified peonidin and malvidin derivatives is reported. Herein, in Table 4 the two-way ANOVA results are presented (considering pre-fermentative treatment—B- and type of

Table 4 LS means from two-way ANOVA results on the percentage (%) of compounds left over in wines with respect to musts

<i>B</i>	463	493	561	505	535	609-1	639-1	609-2	639-2
NF	26.120b	110.405b	143.271a	62.861b	132.428b	139.203b	95.712b	531.603b	91.687a
F	15.197a	63.514a	686.074b	36.235a	34.718a	36.503a	40.223a	48.984a	104.573b
Pr > F(B)	< 0.0001	0.000	0.053	0.040	< 0.0001	< 0.0001	< 0.0001	< 0.0001	0.064
Significant	Yes	Yes	No	Yes	Yes	Yes	Yes	Yes	No
<i>C</i>	463	493	561	505	535	609-1	639-1	609-2	639-2
AMf	23.297b	101.253b	614.852a	66.880b	97.179b	104.400b	78.533b	445.486b	108.381b
Af	18.020a	72.666a	214.493a	32.217a	69.968a	71.307a	57.401a	135.102a	87.879a
Pr > F(C)	0.003	0.005	0.133	0.013	0.011	0.002	0.007	< 0.0001	0.009
Significant	Yes	Yes	No	Yes	Yes	Yes	Yes	Yes	Yes
<i>B*C</i>	463	493	561	505	535	609-1	639-1	609-2	639-2
NF*AMf	30.588c	124.698c	268.917ab	88.474b	161.983c	174.443c	125.468c	843.869c	115.100b
NF*Af	21.652b	96.112bc	17.625a	37.249ab	102.873b	103.963b	65.955b	219.336b	68.273a
F*Af	14.387a	49.221a	411.360ab	27.184a	37.063a	38.650a	48.847ab	50.867a	107.484b
F*AMf	16.007a	77.808b	960.787b	45.286ab	32.374a	34.356a	31.598a	47.102a	101.661b
Pr > F(B*C)	0.018	1.000	0.551	0.166	0.005	0.001	0.000	< 0.0001	0.002
Significant	Yes	No	No	No	Yes	Yes	Yes	Yes	Yes

inoculum—C as factors), showing the related Tukey's HSD groupings.

B pre-fermentative treatment (F frozen, NF non-frozen grapes), *C* type of inoculum (Af alcoholic fermentation, AMf alcoholic + malolactic fermentation), *B*C*, interaction factor.

These results show the extent of the change produced by the pre-fermentative treatment (*B*) and type of inoculum (*C*) factors. All compounds, with the noticeable exception of vitisin A, were significantly higher in wines obtained from non-frozen grapes and in wines subjected to co-inoculation. The interaction *B*C* played a significant role for all compounds, except malvidin-3-glucoside (493), vitisin A (561), and peonidin-3-(6''-acetyl)-glucoside (505). Noteworthy, only 15% of peonidin-3-glucoside was left in wines produced from frozen musts, although this result mainly depended not much on the final concentrations in wine, as much as on the initial higher concentrations in the musts (see Supporting Information—Table SI 2).

To finally highlight also the effects of the application of the fermentative maceration, the related two-way ANOVA analysis on *W* wine samples (wines obtained without fermentative maceration of the grape pomace, and sampled at bottling) are presented in Table 5 (full data in SI—Table SI3).

449 cyanidin-3-glucoside, 463 peonidin-3-glucoside, 465 delphinidin-3-glucoside, 479 petunidin-3-glucoside, 491 cyanidin-3-(6''-acetyl)-glucoside, 493 malvidin-3-glucoside, 505 peonidin-3-(6''-acetyl)-glucoside, 521 petunidin-3-(6''-acetyl)-glucoside, 535 malvidin-3-(6''-acetyl)-glucoside,

561 vitisin A, 609-1 peonidin-3-(6''-cis-*p*-coumaroyl)-glucoside, 609-2 peonidin-3-(6''-trans-*p*-coumaroyl)-glucoside, 625-1 peonidin-3-(6''-caffeoyl)-glucoside, 625-2 petunidin-3-(6''-*p*-coumaroyl)-glucoside, 639-1 malvidin-3-(6''-cis-*p*-coumaroyl)-glucoside, 639-2 malvidin-3-(6''-trans-*p*-coumaroyl)-glucoside; *W* wines obtained without fermentative maceration, F frozen grapes, NF non-frozen grapes, Af inoculum with only yeast, AMf co-inoculum of yeast and malolactic bacteria. LS means and grouping letters are reported only for the significant dependent variables

The interpretation of the results for *W* wines is rather straightforward, much simpler than that for *R* wines (Table 3). Grape freezing caused higher quantities of anthocyanins in the *W_F* wines (wines from frozen grapes), with the exception of few compounds (561, 521, 625-2, 609-2, and 639-2) that were not significantly influenced. The type of inoculum impacted the two major anthocyanins (peonidin-3-glucoside—463, and malvidin-3-glucoside—493), as well as delphinidin-3-glucoside (465), cyanidin-3-glucoside (449), cyanidin-3-(6''-acetyl)-glucoside (491), peonidin-3-(6''-acetyl)-glucoside (505), and peonidin-3-(6''-cis-*p*-coumaroyl)-glucoside (609-1). The interaction term played a role only for malvidin-3-glucoside (493); although the general trend showed higher values in *W_F* wines than *W_NF*, the only samples that were significantly different were those obtained with malolactic fermentation (AMf). Overall, from the comparison between the vinification of white (*W*) and red (*R*) wines, it clearly emerges that the interaction factor played a even

Table 5 Results of the two-way ANOVA and Tukey's HSD for W wines

B	465	449	479	463	493	561	491	521	505	535	625-1	625-2	609-1	609-2	639-2
F	0.101b	0.596a	0.268b	4.998b	9.212b	0.131b	0.131b	0.912b	1.207b	0.732b	0.027b	0.094b	0.094b	0.045b	
NF	0.063a	0.782b	0.136a	4.107a	5.741a	0.097a	0.097a	0.792a	0.497a	0.004a	0.003a	0.041a	0.041a	0.016a	
Pr > F(B)	0.004	0.003	0.011	0.025	<0.0001	0.329	0.031	0.048	<0.0001	<0.0001	0.012	0.000	0.000	0.010	0.078
Significant	Yes	Yes	Yes	Yes	Yes	No	Yes	No	Yes	Yes	Yes	Yes	Yes	No	No
C	465	449	479	463	493	561	491	521	505	535	625-1	625-2	609-1	609-2	639-2
AMf	0.096b	1.021b	5.619b	8.555b	0.139b	0.139b	0.139b	0.912b	1.207b	0.732b	0.027b	0.094b	0.094b	0.045b	
Af	0.067a	0.356a	3.485a	6.397a	0.089a	0.089a	0.089a	0.792a	0.497a	0.004a	0.003a	0.041a	0.041a	0.016a	
Pr > F(C)	0.018	<0.0001	0.382	0.002	0.467	0.005	0.326	0.048	0.983	0.773	0.693	0.003	0.060	0.213	0.997
Significant	Yes	Yes	No	Yes	No	Yes	No	Yes	No	No	No	Yes	No	No	No
B*C	465	449	479	463	493	561	491	521	505	535	625-1	625-2	609-1	609-2	639-2
F*AMf					10.864b										
F*Af					7.559a										
NF*AMf					6.246a										
NF*Af					5.235a										
Pr > F(B*C)	0.471	0.557	0.320	0.400	0.042	0.128	0.905	0.282	0.290	0.960	0.880	0.711	0.639	0.148	0.814
Significant	No	No	No	No	Yes	No	No	No	No	No	No	No	No	No	No

Table 6 N and I values calculated from the spectrophotometrical analysis of the wine samples

Sample	<i>I</i>	Average	St. Dev	<i>N</i>	Average	St. Dev
R_F_Af_A	1.697	1.642	0.198	0.927	0.937	0.053
R_F_Af_B	1.807			0.890		
R_F_Af_C	1.422			0.994		
R_F_AMf_A	1.339	1.410	0.109	1.085	1.084	0.021
R_F_AMf_B	1.535			1.063		
R_F_AMf_C	1.355			1.105		
R_NF_Af_A	1.143	1.160	0.048	0.877	0.861	0.032
R_NF_Af_B	1.214			0.823		
R_NF_Af_C	1.122			0.882		
R_NF_AMf_A	0.843	0.869	0.088	1.087	1.067	0.047
R_NF_AMf_B	0.966			1.014		
R_NF_AMf_C	0.796			1.101		

Table 7 Tukey's HSD test results for I and N parameters

<i>B</i>	<i>I</i>	<i>N</i>
F	1.526b	
NF	1.014a	
Pr > F(B)	< 0.0001	0.080
Significant	Yes	No
<i>C</i>	<i>I</i>	<i>N</i>
Af	1.401 b	0.899 a
AMf	1.139 a	1.076 b
Pr > F(I)	0.006	< 0.0001
Significant	Yes	Yes
<i>B</i> * <i>C</i>	<i>I</i>	<i>N</i>
F*AMf	1.410 c	1.084 b
F*Af	1.642 c	0.937 a
NF*AMf	0.869 a	1.067 b
NF*Af	1.160 b	0.861 a
Pr > F(<i>B</i> * <i>C</i>)	0.000	0.000
Significant	Yes	Yes

B pre-fermentative conditions, *C* type of inoculum, *B***C* interaction term, *F* wines obtained with frozen grapes, *NF* wines obtained from non-frozen grapes, *Af* wines that underwent alcoholic fermentation only, *AMf* wines that underwent alcoholic and malolactic fermentations, *I* colour intensity; *N* colour hue/tint

smaller role for white wine winemaking compared to red wine winemaking. Finally, the trends displayed by the *W* wines obtained with or without grape freezing were in line with the observation made for musts: a higher abundance of anthocyanins (no matter the specific compound) in the samples from frozen grapes.

Spectrophotometric determination of the wines

The measured colour intensity (*I*) and hue/tint (*N*) are reported in Table 6. These parameters have been then

analysed by two-way ANOVA and Tukey's HSD post hoc test to observe directly the effects of the two factors and their interactions (Table 7).

I = colour intensity; *N* = colour hue/tint

The results highlight the effects of the pre-fermentative conditions and the type of inoculum. The use of frozen grapes caused the related wines to be higher in colour intensity, but the hue (*N*) was not significantly different. Malolactic fermentation caused lower colour intensity (*I*) and higher hue/tint values (*N*), thus supporting the hypothesis that malolactic fermentation affected the colouration due to an increase in pH, related to the malic acid–lactic acid conversion (Supporting Information Table SI1).

CIELab colorimetric determination of wines

The results of the colorimetric analysis are reported in Table 8.

A PCA model was built on the presented data (Fig. 5) and the two-way ANOVA results are displayed in Table 9.

B pre-fermentative treatment, *C* type of inoculum, *B***C* interaction term, *L** lightness, *a** red/green coordinate, *b** yellow/blue coordinate, ΔE^* differences in colours, *C** chroma, *H** tone, ΔH^* differences in tones

The largest trend observed in the PCA model is surely the separation of R_NF_AMf samples from the R_F_Af samples. The main separation occurs along PC1, where the R_F_Af samples showed similar scores at high positive values of PC1, whereas the R_NF_AMf samples were clustered on the opposite side of PC1. All other were grouped together in between. Only the *L** variable characterized more R_NF_AMf samples. *C**, *a**, *b**, and all derived parameters (ΔE^* and ΔH^*) characterized more R_F_Af samples. No clear trend associated with the applied study factor could be observed. Therefore, to clarify the relation between these trends and the applied study factors, a two-way ANOVA was applied (Table 9).

Table 8 L^* , a^* , b^* , C^* and derived values ΔE^* and ΔH^* calculated for the colorimetric analysis of the wine samples

Sample	<i>B</i>	<i>C</i>	L^*	a^*	b^*	ΔE^*	C^*	H^*	ΔH^*
R_F_Af_A	F	Af	47.1	9.1	4.6	12.4	10.2	27.0	4.3
R_F_Af_B	F	Af	47.0	9.8	4.9	13.0	10.9	26.3	4.4
R_F_Af_C	F	Af	47.0	9.4	4.7	12.7	10.6	26.7	4.3
R_F_AMf_A	F	AMf	47.2	8.0	4.5	11.5	9.1	29.3	4.3
R_F_AMf_B	F	AMf	47.4	8.3	4.7	11.7	9.5	29.4	4.4
R_F_AMf_C	F	AMf	47.7	8.2	4.2	11.2	9.5	30.8	3.4
R_NF_Af_A	NF	Af	47.4	8.2	4.0	11.4	9.2	26.5	4.0
R_NF_Af_B	NF	Af	47.6	9.0	3.5	11.5	9.7	21.3	3.7
R_NF_Af_C	NF	Af	47.2	7.4	4.6	11.3	8.7	31.7	4.4
R_NF_AMf_A	NF	AMf	48.6	6.5	3.3	9.1	7.2	27.0	3.8
R_NF_AMf_B	NF	AMf	49.7	6.2	3.3	8.4	7.0	27.6	3.8
R_NF_AMf_C	NF	AMf	50.8	6.0	3.2	7.7	6.8	28.2	3.8

B pre-fermentative treatment, *C* type of inoculum, *F* wines from frozen grapes, *NF* wines from non-frozen grapes, *Af* wines obtained with alcoholic fermentation only, *AMf* wines obtained with alcoholic and malolactic fermentations, L^* lightness, a^* red/green coordinate, b^* yellow/blue coordinate, ΔE^* differences in colours, C^* chroma, H^* tone, ΔH^* differences in tones

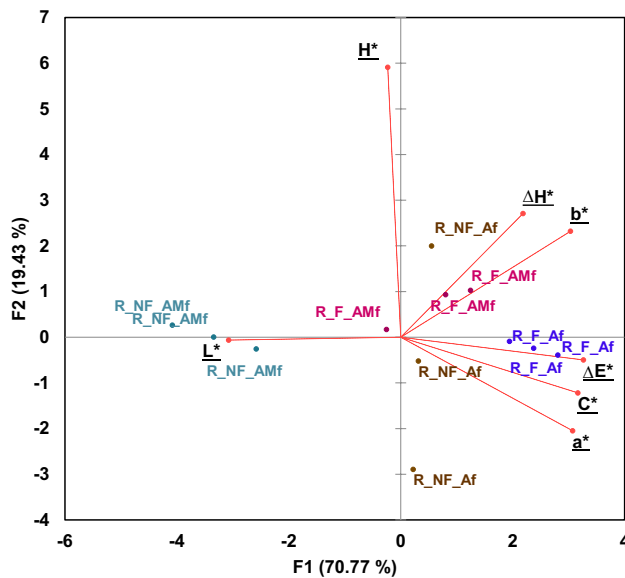


Fig. 5 PCA model biplot for wines (at bottling) built on colorimetric parameters. *R* must that subsequently underwent fermentative maceration. *R* wines that underwent fermentative maceration, *NF* wines from non-frozen grapes, *F* wines from frozen grapes, *Af* wines that underwent alcoholic fermentation only, *AMf* wines that underwent alcoholic and malolactic fermentations, C^* chroma, L^* lightness, H^* tone, ΔE^* differences in colours, ΔH^* differences in tones, a^* red/green coordinate, b^* yellow/blue coordinate

The presented two-way ANOVA highlighted the effect of the applied factors on the colour in wine. Pre-fermentative grape freezing (samples *F*) resulted in wines with lower lightness than *NF* samples, which were significantly higher in a^* and b^* (so, more red and yellow coloured) than *NF* samples. The same effects were observed with *Af* samples in comparison to *AMf* samples. *Af* samples

were lower in lightness (L^*) and higher in red and yellow than *AMf* samples. Overall, this resulted in *F_Af* samples to be the highest in a^* and b^* , whereas *NF_AMf* were the highest in L^* . The same trend was present also in Chroma C^* and colour difference ΔE^* , as these were significantly higher in *F_Af*, and lowest in *NF_AMf*; for the other samples (*F_AMf* and *NF_Af*), they showed intermediate and non-significantly different values. This is an interesting observation, as it shows that the application of grape freezing and malolactic fermentation co-operated to make these two seemingly different samples quite close in colour parameters. In any case, the conditions that allowed the wines to retain the highest colour at bottling were grape freezing without co-inoculum of malolactic bacteria. This effect could be only partially associated with the observed anthocyanins' profile. Indeed, peonidin-3-glucoside showed significantly higher concentrations in wines from frozen grapes (malvidin-3-glucoside was equally more concentrated in *F* wines, but with no significant difference); however, the less concentrated anthocyanins were almost all more concentrated in *NF* samples. pH, a major parameter influencing colour, showed a distinct effect with respect to grape freezing (Supporting Information Table S11), as well as the measured alcohol by volume ($\%_{ABV}$), which was higher in all *F* samples than *NF* samples. The higher pH in *F* samples causes the precipitation of tartaric salts, which is accelerated at low temperatures. The lower amount of tartaric acid in *F* wines (reported in Table S11) could be imputed to this factor.

Table 3 shows that the concentration of anthocyanin peonidin-3-glucoside in wine was positively influenced by grape freezing, whereas malvidin-3-glucoside was mostly unaffected and most of the other compounds (albeit lower in quantity) were negatively affected. Malolactic fermentation

Table 9. Two-way ANOVA with Tukey’s groups on the colorimetric parameters shown in Table 5

	<i>B</i>	<i>L</i> *	<i>a</i> *	<i>b</i> *	ΔE^*	<i>C</i> *	<i>H</i> *	ΔH^*
F		47.240 a	8.796 b	4.591 b	12.099 b	9.983 b	28.257 a	4.167 a
NF		48.543 b	7.215 a	3.648 a	9.904 a	8.103 a	27.058 a	3.895 a
Pr>F(B)		0.004	0.000	0.001	<0.0001	<0.0001	0.455	0.193
Significant		Yes	Yes	Yes	Yes	Yes	No	No
<i>C</i>								
Af		47.198 a	8.830 b	4.395 b	12.054 b	9.885 b	26.590 a	4.174 a
AMf		48.585 b	7.181 a	3.843 a	9.949 a	8.200 a	28.724 a	3.887 a
Pr>F(C)		0.003	0.000	0.011	<0.0001	<0.0001	0.200	0.172
Significant		Yes	Yes	Yes	Yes	Yes	No	No
<i>B</i> * <i>C</i>								
F*Af		47.030 a	9.445 c	4.745 b	12.713 c	10.575 c	26.680 a	4.324 b
F*AMf		47.450 b	8.147 b	4.437 b	11.484 b	9.390 b	29.833 a	4.009 ab
NF*Af		47.365 ab	8.215 bc	4.045 ab	11.395 b	9.195 b	26.500 a	4.024 ab
NF*AMf		49.720 c	6.215 a	3.250 a	8.414 a	7.010 a	27.615 a	3.766 a
Pr>F(B*C)		0.018	0.233	0.188	0.007	0.040	0.523	0.886
Significant		Yes	No	No	Yes	Yes	No	No

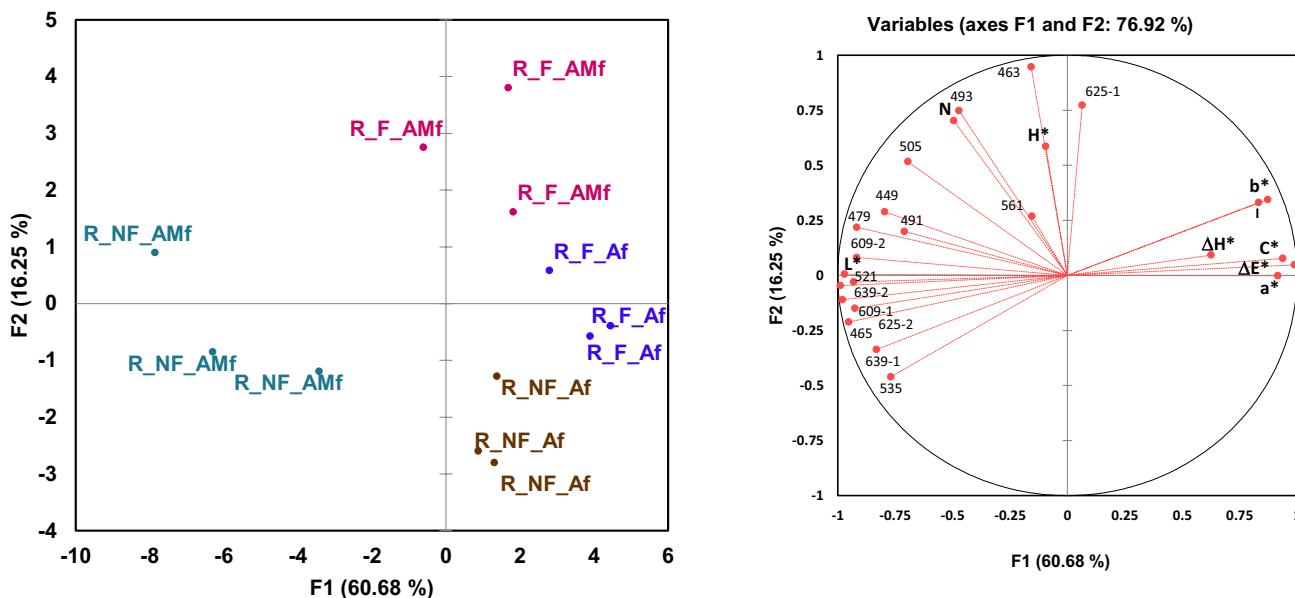


Fig. 6 PCA biplot (auto-scaled variables) for R wines at bottling built on anthocyanins and colorimetric parameters. Left plot—scores plot; right plot—loadings plot. R wines that underwent fermentative maceration, NF wines from non-frozen grapes, F wines from frozen grapes, Af wines that underwent alcoholic fermentation only, AMf

wines that underwent alcoholic and malolactic fermentations, N hue/tint, I colour intensity, C* chroma, L* lightness, H* tone, ΔE* differences in colours, ΔH* differences in tones, a* red/green coordinate, and b* yellow/blue coordinate

(co-inoculum) did positively influence the extraction of most anthocyanins (including peonidin-3-glucoside) from the grape skins, albeit it produced wines with lower a*, b*, and ΔE* parameters. The anthocyanins and spectrophotometric and colorimetric profiles of the investigated R wines were also analysed together using PCA (Fig. 6).

Additional information can be derived by the PCA in Fig. 6. Here, the separation between AMf and Af samples,

as well as the separation between F and NF samples, are well shown than in Fig. 5. The two trends (separation of AMf from Af vs the separation between NF and F) are almost perpendicular (diagonally with respect to the PCs components). This means that the combination of all the presented parameters (colorimetric, spectrophotometric, and chemical) allows to build a multivariate model able to separate and

highlight the effects of the two main factors under study on the samples and in relation to the measured parameters.

Specifically, the main separation is shown between R_NF_AMf and R_F_Af samples (on opposite sides of PC1), exactly as in the PCA in Fig. 5. The other sets of samples (R_NF_Af and R_F_AMf) are located in between, at intermediate values of PC1. The spectrophotometric I (intensity) parameter appears highly correlated to the colorimetric b^* (yellow/blue coordinate) and slightly with the colorimetric a^* (red/green coordinate), whereas N is not strongly correlated with any colorimetric parameter. Instead, N shows a high correlation to malvidin-3-glucoside (493) and to some extent with vitisin A (561).

Besides, the main trend of these parameters occurs along PC1, with the exception of H^* . Notably, L^* appears anti-correlated to most of the other parameters (I , a^* , b^* , ΔE^* , ΔH^* , and C^*). As mentioned in comments to Fig. 5, F_AMf and NF_Af are similar with respect to the colorimetric parameters, with the exception of H^* . Indeed, they show similar scores along the PC1 component in Fig. 6. At the same time, the H^* parameter was not significantly different according to ANOVA (Table 9), albeit F_AMf condition showed higher concentrations of the main monoglucosidic anthocyanins. As seen above (Table 3), PCA showed that monoglucosidic anthocyanins were significantly higher in F samples only for peonidin-3-glucoside (463), which was positively correlated with parameter H^* . On the contrary, delphinidin and petunidin-3-glucoside (465 and 479, respectively) were higher in NF samples, which were positively correlated with the L^* parameter. On the contrary, malvidin-3-glucoside (493), which was positively correlated with the N parameter, was not significantly different between the R_F and R_NF samples. AMf samples presented higher significant values for all monoglucosides. The derived species (acylated, *p*-coumaroylated, etc.) were generally higher in the NF samples, with few exceptions (peonidin-3-(6'-acetyl)-glucoside (505) and peonidin-3-(6''-caffeoyl)-glucoside (625-1)) that were positively correlated with the H^* and N parameters. Conversely, AMf vs Af samples showed similar trends for the derived pigments than the monoglucosides (higher values in AMf samples), with the exception of malvidin-3-(6'-acetyl)-glucoside (535). All other spectrophotometric and colorimetric parameters were anti-correlated to most derived pigments (acylated, *p*-coumaroylated, etc.), which in turn showed the highest correlations with L^* (lightness). It may also be observed that a^* , B^* , C^* , and ΔE^* parameters seem to be mostly associated to the F samples in Fig. 6, whereas L^* has the lowest association with F_Af and NF_Af. H^* is mostly associated with F_AMf and strongly correlated to 463 (peonidin-3-glucoside).

This apparently contradictory result, i.e. the anti-correlation between most colorimetric parameters and the largest number of anthocyanin species, was further investigated.

Firstly, it is noticeable that pH values (Supporting Information—Table S1) are widely different for the four type of R samples investigated in this study. The pH (± 0.1) values are 3.5, 3.7, 3.3 and 3.4 for (R) F_Af, F_AMf, NF_Af and NF_AMf, respectively. The samples that underwent grape freezing had the highest pH values (up to 3.7 for F_AMf samples). Combining grape freezing and malolactic fermentation caused a decrease in the content of organic acids due to precipitation (the former), and an increase in pH due to malic acid–lactic acid conversion (the latter). The derived anthocyanins species (acylated, *p*-coumaroylated, etc.) are still under investigation because the diverse patterns of methoxylation, hydroxylation, glycosylation, and acylation can have an effect on the overall resulting expressed colour [35]. The L^* (lightness) and C^* (chroma) values are influenced by the concentration of the compounds in the sample; however, pH, presence of co-pigments, and structural modifications (e.g. acylation) can influence the colorimetric outcomes, leading to differences in the L^* and C^* parameters. In particular, acylation is known to cause a decrease in L^* and an increase in C^* , resulting in a darker and more intense sample, but these changes are pH dependent [35]. Furthermore, the *cis* isomer shows a decrease in L^* and an increase in C^* at acidic pH. In contrast, the *trans* isomer, which is predominant in nature [32], shows an increase in L^* and a decrease in C^* . In fact, our results shows that the *trans* isomers (609-2 and 639-2) were strongly positively correlated with L^* and negatively correlated with C^* ; moreover, their amount was higher in the R_NF_AMf samples followed by the *cis* isomers (609-1 and 639-1). In contrast, the F samples were positively correlated with C^* . Thus, the R_NF samples that underwent alcoholic and malolactic fermentation had a larger accumulation of most of the minor anthocyanin derivatives [35]. Once again, the PCA (Fig. 6) showed that the accumulation of all anthocyanins correlated positively with the application of malolactic fermentation, as confirmed by the ANOVA results (Table 3). Another viewpoint, the presence of unaccounted-for oligomeric pigments (e.g. anthocyanin adducts with flavan-3-ols) could have been a possible explanation for these discrepancies, but this hypothesis was discarded, as these compounds were not observed by the analysis of LC-PDA and HPLC–MS traces (*data not shown*). It is well known that co-pigmentation is affected by pH [7, 8]. A combination of pH and abundance of grape-extracted co-pigmentation species (e.g. cinnamic acid) might explain the observed trends. An increased amount of co-pigments along with higher pH might overcome a lower content of anthocyanins in producing higher pigmentations anyway.

To tentatively address this hypothesis, the extracted PDA chromatograms at 280 nm and 320 nm are reported (Supporting Information—Table SI6 and Table SI7); for each sample, the ratios between the two chromatograms at 320 and 280 nm are presented (Supporting Information Table

SI8). Indeed, as flavonols (e.g. kaempferol, quercetin, myricetin), dihydroflavonols (e.g. astilbin and taxifolin), and cinnamic acids (e.g. *p*-coumaric, *trans*-caffeic, ferulic etc.) have spectral relative maxima near or higher of 310 nm, their peaks show higher $\text{Abs}^{320\text{ nm}}/\text{Abs}^{280\text{ nm}}$ values than other phenols (e.g. hydroxybenzoic acids, flavan-3-ols, etc.). Some of these species are considered very strong co-pigments in wine [36, 37]. A PCA model was built taking the entire dataset of $\text{Abs}^{320\text{ nm}}/\text{Abs}^{280\text{ nm}}$ derived traces (Supporting Information—Table SI9). The PCA on this dataset separated neatly all the four R samples. The ranges of retention times (loadings) in any sample presenting higher $\text{Abs}^{320\text{ nm}}/\text{Abs}^{280\text{ nm}}$ ratios values were further filtered by parallel inspection of the LC–PDA–MS traces. Identified peaks along with their tentative assignments based on full MS spectra, MS^2 fragmentation, and UV–Vis spectral $\lambda_{\text{max}} > 310\text{ nm}$, are reported in the Supporting Information—Table SI11.

The PCA was then re-calculated based on the selection of these variables (Supporting Information—Table SI10). R_F samples were characterized by a higher contribution of only the compounds at 11.6 min and tentatively assigned full MS ions m/z 487.1 and m/z 303.1, which showed a λ_{max} at 355 nm. R_AMf samples were completely separated on the other side of PC1, and characterized by higher relative abundances of all other species, besides the compound at 14.1 min (tentatively, m/z 561, m/z 501, and m/z 317), with a λ_{max} at 340 and 280 nm. The NF_AMf samples were characterized by higher contributions of all other compounds, except m/z 487.1 at 11.6 min. Besides, PC2 vs PC3 showed a separation along the diagonal (from left to right) of NF_Af, F_Af, NF_AMf, and F_AMf, progressively.

The PC1 vs PC2 score plot in Supporting Information Table SI10 built on these chemical variables resembles the PC1-inverted scores plot arrangement for colorimetric parameters (Fig. 7), indicating a possible relationship between the two profiles. In these respects, the compound at 11.6 min (full MS: m/z 487; MS^2 product ions—40 eV: m/z 487, m/z 333, m/z 325, m/z 310, m/z 254; see Supporting Information—Table SI11) would show the same trend of the parameter a^* , b^* , ΔE^* , C^* and ΔH^* observed from the two-way ANOVA (Table 9).

Conclusion

This study contributes to a greater understanding of the effects of co-inoculum of yeasts and malolactic bacteria and that of pre-fermentative grape freezing on the vinification of a red grape variety (Schiava cv.), which is prone to rapid loss in colour. These findings could be useful to winemakers in general to better understand the change in the pigments profile, when using grape varieties that are higher in B-ring disubstituted anthocyanins compared to trisubstituted ones,

which may be a cause for colour instability. Higher extraction in most of the major anthocyanin peonidin-3-glucoside was correlated to the application of grape freezing; however, this did not translate into a higher concentration absolutely in all the related wines, and the relative drop in concentration for peonidin-3-glucoside from the musts was of 85% and 75% in F and NF wines, respectively. Besides, the amount of all anthocyanins except peonidin-3-glucoside and malvidin-3-glucoside were lower in wines from frozen grapes than in control wines. Wines obtained with co-inoculation showed anyway higher anthocyanin content than in wine without applied malolactic fermentation. Petunidin-3-(6''-*p*-coumaroyl)-glucoside, peonidin-3-(6''-*cis*-*p*-coumaroyl)-glucoside and malvidin-3-(6''-*trans*-*p*-coumaroyl)-glucoside were dramatically affected by the interaction of the two applied factors. Peonidin-3-(6'-caffeoyl)-glucoside increased over the fermentation in all these although it showed a drop between the end of the fermentation and the wine bottling. Malvidin-3-glucoside showed a completely different dependence on time and the type of vinification than peonidin-3-glucoside: it did not show differences for wines from frozen or non-frozen grapes, and it showed either a much slower decrease over the fermentation than its peonidin-containing analogues, or even an overall increase. Overall, the wines from frozen grapes that underwent malolactic fermentation besides the main alcoholic fermentation were the ones with the highest residual peonidin-3-glucoside and malvidin-3-glucoside. Then, an interesting relation between the abundances of four major anthocyanidins monoglucosides (cyanidin, petunidin, peonidin, and malvidin) in must from frozen grapes was observed. In these musts, the same ratio was found for malvidin-3-glucoside/peonidin-3-glucoside and for petunidin-3-glucoside/cyanidin-3-glucoside. The same relations were not found in musts from non-frozen grapes. This observation may indicate that grape freezing effectively allows a complete extraction of the anthocyanins monoglucosides from the grapes, overcoming the differences in extractability. However, more investigation will be required to fully elucidate this phenomenon. Regarding the colorimetric parameters, H^* (colorimetric hue) was strongly correlated with peonidin-3-glucoside and spectrophotometric tint (N) with malvidin-3-glucoside. Tint also showed a positive correlation with the application of the malolactic fermentation. Some minor pigment compounds showed opposite trends. Regarding the colorimetric parameters of wine, a^* (red/green), b^* (yellow/blue), ΔE^* (differences in color), C^* (chroma), H^* (tone), ΔH^* (differences in tone) correlated with the application of grape freezing and inversely to the application of malolactic fermentation. L^* (lightness) instead showed higher values in wines from non-frozen grapes with applied malolactic fermentation. A potential relation of these findings with the effect of grape freezing and malolactic fermentation on the pH and with

the presence of potential co-pigmentation species has been discussed.

In the literature, this type of studies have focused on grape varieties with a larger impact on the winemaking sector. However, it should be considered that minor grape varieties are a fundamental part of the enological tradition of many countries and regions, and a strive to preserve and improve the regional biodiversities is ongoing, also in agreement with current EU agricultural policies. This study offers also an experimental example on how vinifications can be planned to obtain different styles of wine from the same grapes and allows the winemaker subsequently to create blends of them, to provide even more tools for obtaining the desired wine style. In this regard, the process of colour assessment in red and rosé wines is a fundamental step for defining the wine quality. Other factors, such as the extraction technique, the abundance and type of co-pigments and the stability of the co-pigmentation complexes played an even greater role in influencing the colour, besides the abundance of anthocyanins itself [38–40].

Supplementary Information The online version contains supplementary material available at <https://doi.org/10.1007/s00217-023-04270-5>.

Acknowledgements We warmly thank Hartmann Donà (Lana, South Tyrol, Italy) for providing the grapes used in this study. The publication of this work is supported by the Open Access Publishing Fund of the Free University of Bozen-Bolzano.

Author contributions AD: investigation, data curation, formal analysis, writing—review and editing; SP: conceptualization, software, investigation, data curation, writing—review and editing; ATC: conceptualization, validation, formal analysis, writing—review and editing; TM: resources, funding acquisition; EB: resources, supervision, funding acquisition; EL: conceptualization, methodology, validation, formal analysis, investigation, data curation, writing—original draft, writing—review and editing, visualization, project administration, funding acquisition.

Funding Open access funding provided by Libera Università di Bolzano within the CRUI-CARE Agreement. This work was supported by the grant TN202D of the Free University of Bozen-Bolzano, and by the AMARE Capacity building fund from the Autonomous Province of Bozen/Bolzano.

Data availability All the data collected in this study have been made available in the provided supporting information, and are also available upon request to the corresponding author.

Declarations

Conflict of interest The authors declare no known competing financial interests or conflict of interests that could have influenced the work reported in this paper.

Compliance with ethics requirements This study does not contain any studies with human participants or animals performed by any of the authors.

Open Access This article is licensed under a Creative Commons Attribution 4.0 International License, which permits use, sharing,

adaptation, distribution and reproduction in any medium or format, as long as you give appropriate credit to the original author(s) and the source, provide a link to the Creative Commons licence, and indicate if changes were made. The images or other third party material in this article are included in the article's Creative Commons licence, unless indicated otherwise in a credit line to the material. If material is not included in the article's Creative Commons licence and your intended use is not permitted by statutory regulation or exceeds the permitted use, you will need to obtain permission directly from the copyright holder. To view a copy of this licence, visit <http://creativecommons.org/licenses/by/4.0/>.

References

1. Castañeda-Ovando A, de Lourdes P-HM, Páez-Hernández ME, Rodríguez JA, Galán-Vidal CA (2009) Chemical studies of anthocyanins: a review. *Food Chem*. 113(4):859–871
2. Andersen ØM, Jordheim M (2006) The Anthocyanins. In: Andersen ØM, Markham KR (eds) *Flavonoids chemistry, biochemistry and applications*. CRC Press Taylor and Francis, Boca Raton, pp 471–551
3. Konczak I, Zhang W (2004) Anthocyanins—more than nature's colours. *J Biotechnol Biomed* 2004(5):239
4. Pojer E, Mattivi F, Johnson D, Stockley CS (2013) The case for anthocyanin consumption to promote human health: a review. *CRFSFS* 12(5):483–508
5. Li D, Wang P, Luo Y, Zhao M, Chen F (2017) Health benefits of anthocyanins and molecular mechanisms: update from recent decade. *Crit Rev Food Sci Nutr* 57(8):1729–1741
6. Arapitsas P, Oliveira J, Mattivi F (2015) Do white grapes really exist? *Food Res Int* 69:21–25
7. Boulton R (2001) The co-pigmentation of anthocyanins and its role in the color of red wine: a critical review. *AJEV* 52(2):67–87
8. Robinson GM, Robinson R (1931) A survey of anthocyanins. *I Biochem J* 25(5):1687
9. Boselli E, Boulton RB, Thorngate JH, Frega NG (2004) Chemical and sensory characterization of DOC red wines from Marche (Italy) related to vintage and grape cultivars. *J Agric Food Chem* 52(12):3843–3854
10. Dangles O, Fenger JA (2018) The chemical reactivity of anthocyanins and its consequences in food science and nutrition. *Molecules* 23(8): 1970.
11. Zhao X, Zhang N, He F, Duan C (2022) Reactivity comparison of three malvidin-type anthocyanins forming derived pigments in model wine solutions. *Food Chem* 384:132534
12. Liu Y, Zhang XK, Shi Y, Duan CQ, He F (2019) Reaction kinetics of the acetaldehyde-mediated condensation between (–)-epicatechin and anthocyanins and their effects on the color in model wine solutions. *Food Chem* 283:315–323
13. Jordheim M, Fossen T, Songstad J, Andersen ØM (2007) Reactivity of anthocyanins and pyranoanthocyanins. Studies on aromatic hydrogen–deuterium exchange reactions in methanol. *J Agric Food Chem* 55(20): 8261–8268.
14. Mattivi F, Scienza A, Failla O, Villa P, Anzani R, Tedesco G, Gianazza E, Righetti P (1990) *Vitis vinifera*—a chemotaxonomic approach: anthocyanins in the skin. In: 5th International symposium on grape breeding, 119–133
15. Arapitsas P, Ugliano M, Marangon M, Piombino P, Rolle L, Gerbi V, Versari A, Mattivi F (2020) Use of untargeted liquid chromatography–mass spectrometry metabolome to discriminate Italian monovarietal red wines, produced in their different terroirs. *J Agric Food Chem* 68(47):13353–13366
16. Pereira GK, Donate PM, Galembeck SE (1997) Effects of substitution for hydroxyl in the B-ring of the flavylium cation. *J Mol Struct Theochem* 392:169–179

17. Baranac J, Amic D, Vukadinovic V (1990) Spectrophotometric study of the influence of individual substituted positions on flavylum chromophore stability. *J Agric Food Chem* 38(4):932–936
18. Mattioli R, Francioso A, Mosca L, Silva P (2020) Anthocyanins: a comprehensive review of their chemical properties and health effects on cardiovascular and neurodegenerative diseases. *Molecules* 25:3809
19. Unterkofler J, Muhlack RA, Jeffery DW (2020) Processes and purposes of extraction of grape components during winemaking: current state and perspectives. *Appl Microbiol Biotechnol* 104(11):4737–4755
20. Sacchi KL, Bisson LF, Adams DO (2005) A review of the effect of winemaking techniques on phenolic extraction in red wines. *AJEV* 56(3):197–206
21. Segade SR, Pace C, Torchio F, Giacosa S, Gerbi V, Rolle L (2015) Impact of maceration enzymes on skin softening and relationship with anthocyanin extraction in wine grapes with different anthocyanin profiles. *Food Res Int* 71:50–57
22. Burns TR, Osborne JP (2015) Loss of Pinot noir wine color and polymeric pigment after malolactic fermentation and potential causes. *AJEV* 66(2):130–137
23. Ribereau-Gayon P, Dubourdiou D, Doneche BA, Lonvaud A (2006) Handbook of enology volume 1: the microbiology of wine and vinifications, 2nd Edition. Wiley (ISBN:0-470-01034-7)
24. Romero-Cascales I, Fernández-Fernández JI, López-Roca JM, Gómez-Plaza E (2005) The maceration process during winemaking extraction of anthocyanins from grape skins into wine. *Eur Food Res Technol* 221:163–167
25. OIV (2023) Compendium of International Analysis of Methods-OIV. In: Resolution 2009. Chromatic Characteristics. Type IV methods. Method OIV-MA-AS2–07B
26. Mazza G, Fukumoto L, Delaquis P, Girard B, Ewert B (1999) Anthocyanins, phenolics, and color of cabernet franc, merlot, and pinot noir wines from british columbia. *J Agric Food Chem* 47(10):4009–4017
27. OIV (2023) Compendium of International Analysis of Methods-OIV. In: Resolution Oeno 1/2006. Determination of chromatic characteristics according to CIELab – Type I methods. Method OIV-MA-AS2–11
28. OIV (2023) Compendium of International Analysis of Methods-OIV. In: Resolution Oeno 566/2016. Alcoholic strength by volume – Type I methods. Method OIV-MA-AS312–01A
29. Blanco-Vega D, López-Bellido FJ, Alía-Robledo JM, Hermosín-Gutiérrez I (2011) HPLC–DAD–ESI–MS/MS characterization of pyranoanthocyanins pigments formed in model wine. *J Agric Food Chem* 59(17):9523–9531
30. Favre G, Hermosín-Gutiérrez I, Piccardo D, Gómez-Alonso S, González-Neves G (2019) Selectivity of pigments extraction from grapes and their partial retention in the pomace during red-winemaking. *Food Chem* 277:391–397
31. Arapitsas P, Perenzoni D, Nicolini G, Mattivi F (2012) Study of sangiovese wines pigment profile by UHPLC–MS/MS. *J Agric Food Chem* 60(42):10461–10471
32. Hayasaka Y, Asenstorfer RE (2002) Screening for potential pigments derived from anthocyanins in red wine using nano-electrospray tandem mass spectrometry. *J Agric Food Chem* 50(4):756–761
33. Francia-Aricha EM, Guerra MT, Rivas-Gonzalo JC, Santos-Buelga C (1997) New anthocyanin pigments formed after condensation with flavanols. *J Agric Food Chem* 45(6):2262–2266
34. Makila L, Laaksonen O, Alanne AL, Kortensniemi M, Kallio H, Yang B (2016) Stability of hydroxycinnamic acid derivatives, flavonol glycosides, and anthocyanins in black currant juice. *J Agric Food Chem* 64(22):4584–4598
35. Sigurdson GT, Tang P, Giusti MM (2018) *Cis*–*trans* configuration of coumaric acid acylation affects the spectral and colorimetric properties of anthocyanins. *Molecules* 23(3):598
36. Bimpilas A, Panagopoulou M, Tsimogiannis D, Oreopoulou V (2016) Anthocyanin co-pigmentation and color of wine: the effect of naturally obtained hydroxycinnamic acids as cofactors. *Food Chem* 197:39–46
37. Marchi D, Lanati D, Mazza G, Cascio P (2019) Composizione in antociani e flavonoli di vini prodotti nel territorio svizzero. In: BIO Web of Conferences vol. 15, EDP Sciences, pp 02012.
38. Heras-Roger J, Díaz-Romero C, Darias-Martín J (2016) What gives a wine its strong red color? Main correlations affecting co-pigmentation. *J Agric Food Chem* 64(34):6567–6574
39. Trouillas P, Sancho-García JC, De Freitas V, Gierschner J, Otyepka M, Dangles O (2016) Stabilizing and modulating color by co-pigmentation: Insights from theory and experiment. *Chem Rev* 116(9):4937–4982
40. Boselli E, Giomo A, Minardi M, Frega NG (2008) Characterization of phenolics in Lacrima di Morro d’Alba wine and role on its sensory attributes. *EFRT* 227(3):709–720

Publisher's Note Springer Nature remains neutral with regard to jurisdictional claims in published maps and institutional affiliations.